An Approximate Message Passing Algorithm for Channel and Impulsive Noise Estimation in Underwater Acoustic OFDM Systems

Shuyi Wu*, Shuche Wang*, Zhiqiang He*, Kai Niu*, and Yue Rong†
*Key Laboratory of Universal Wireless Communications, Ministry of Education,
Beijing University of Posts and Telecommunications (BUPT), Beijing, China
†School of Electrical Engineering, Computing and Mathematical Sciences, Curtin University, Bentley, WA 6102, Australia

***Abstract*—An accurate and efficient channel and impulsive noise estimation is an important step in underwater acoustic (UA) orthogonal frequency-division multiplexing systems. We propose an approximate message passing (AMP) algorithm for channel and impulsive noise estimation. In particular, we model the distribution of the channel impulse response and impulsive noise as a Gaussian mixture, which is the prior information for the AMP algorithm. The proposed algorithm is evaluated through numerical simulations and real data collected during a UA communication experiment conducted in December 2015 in the estuary of the Swan River, Western Australia. The simulation and experimental results show that compared with existing approaches, the proposed algorithm has a better performance.**

I. Introduction

The underwater acoustic (UA) channel is one of the most complicated time-varying channels with significant Doppler spread and strong multipath interference [1], [2]. To mitigate the inter-symbol interference (ISI) caused by multipath propagation, the orthogonal frequency-division multiplexing (OFDM) technique is widely used in UA communication systems. However, it has been reported that impulsive noise generated by natural sources and human activities [3], [4] can significantly degrade the performance of UA OFDM systems [5].

Recently, various approaches have been proposed to mitigate impulsive noise by utilizing the characteristics of impulsive noise. Compared with additive white Gaussian noise (AWGN), impulsive noise has shorter duration and higher power. Thus, the locations of impulsive noise can be obtained by threshold testing, and blanking or clipping based methods can be used to eliminate impulsive noise [6]. However, a drawback of these methods is that they may remove or distort useful signals. Alternatively, by utilizing the structure of OFDM systems and the sparsity of UA channel and impulsive noise, channel estimation and impulsive noise removal methods have been proposed [7]-[11]. It has been shown in [9] that the joint channel and impulsive noise estimation algorithm outperforms conventional clipping-blanking and least-squares (LS) based algorithms.

In this paper, we propose a novel channel and impulsive noise estimation algorithm based on the approximate message passing (AMP) method. In particular, we model the distribution of the channel impulse response and impulsive noise as a Gaussian mixture (GM), which is the prior information for the generalized AMP (GAMP) algorithm [12], [13]. The expectation maximization (EM) algorithm is applied to learn the parameters of the distribution. Firstly, the proposed algorithm is applied to estimate the impulsive noise. Then, we subtract the estimated impulsive noise from the received signals. Since the influence of impulsive noise is reduced, the UA channel can be more accurately estimated by the proposed algorithm. Finally, an iterative process is proposed to further improve the accuracy of channel and impulsive noise estimation.

The performance of the proposed algorithm is evaluated by numerical simulations and real data collected during a UA communication experiment conducted in December 2015 in the estuary of the Swan River, Western Australia. The simulation and experimental results show that the proposed algorithm can effectively mitigate impulsive noise and achieve a better system bit-error-rate (BER) and frame-error-rate (FER) performance. Compared with the existing algorithms, the proposed algorithm can significantly improve the performance of UA OFDM systems.

The rest of the paper is organized as follows. The system model is introduced in Section II. The proposed channel and impulsive noise estimation approach is presented in Section III. Numerical simulation and experimental results are shown in Section IV and Section V, respectively. Conclusions are drawn in Section VI.

II. System Model

We consider a turbo coded OFDM system [9]. The source signals are transmitted through the UA channel after coding, modulation, and inverse discrete Fourier transform (DFT). Among the total N_c subcarriers, there are N_s data subcarriers, N_p uniformly distributed pilot subcarriers, N_f subcarriers for carrier frequency offset (CFO) estimation, and N_n null subcarriers at both edges of the passband. In each frame, through encoding, interleaving, and code puncturing, a binary source data stream $\mathbf{b}$ is transformed to a coded sequence $\mathbf{c}$ with length $L_c = R_m N_s N_b$, where R_m denotes the modulation order and N_b is the number of OFDM blocks in one frame. The coded sequence $\mathbf{c}$ is mapped into $N_s N_b$ data symbols taken from the quadrature phase-shift keying (QPSK) or quadrature amplitude modulation (QAM) constellations. The N_p pilot subcarriers are modulated by QPSK constellations. To avoid interference among OFDM blocks, a cyclic prefix (CP) is inserted in front of each OFDM symbol. The length of one OFDM block is $T_{total} = T_{sc} + T_{cp}$, where T_{sc} is the length of one OFDM symbol and T_{cp} is the length of the CP. The

978-1-7281-1450-7/19/$31.00 ©2019 IEEE

subcarrier spacing is $f_{sc} = 1/T_{sc}$ and the bandwidth of the transmitted signals is $B = f_{sc}N_c$.

As this paper studies channel and impulsive noise estimation, we consider that the CFO is properly estimated and compensated. Therefore, after downshifting, low-pass filtering, sampling, and removing the CP, the time domain and frequency domain received signals can be written in vector forms as

$$\mathbf{r} = \mathbf{F}^H\mathbf{D}\mathbf{F}\mathbf{h}_t + \mathbf{v}_t + \mathbf{w}_t \tag{1}$$

$$\mathbf{r}_f = \mathbf{D}\mathbf{h}_f + \mathbf{v}_f + \mathbf{w}_f \tag{2}$$

where $\mathbf{D} = \mathrm{diag}(\mathbf{d})$ is a diagonal matrix taking $\mathbf{d}$ as the main diagonal elements, $\mathbf{d}$ is the transmitted OFDM symbol vector, $\mathbf{v}_t$ and $\mathbf{w}_t$ are the time domain impulsive noise and the background Gaussian noise vectors, respectively, $\mathbf{h}_t$ denotes the time domain channel impulse response, $\mathbf{F}$ is an $N_c \times N_c$ normalized DFT matrix, $\mathbf{h}_f = \mathbf{F}\mathbf{h}_t$, $\mathbf{v}_f = \mathbf{F}\mathbf{v}_t$, $\mathbf{w}_f = \mathbf{F}\mathbf{w}_t$, and $(\cdot)^H$ stands for Hermitian transpose.

III. The Proposed Approach

In this section, the GAMP algorithm is applied to estimate the channel and impulsive noise. We assume that the impulsive noise and channel impulse response follow the GM model. Then, the GAMP algorithm is used to estimate the posteriors of the impulsive noise and the channel impulse response. The EM method is applied to compute the optimal parameters in the posteriors. In order to reduce the impact of impulsive noise, the estimated impulsive noise is subtracted from the received signals before the channel estimation.

The received signal on the pilot subcarriers can be obtained from (2) as

$$\mathbf{r}_p = \mathbf{P}\mathbf{D}\mathbf{F}\mathbf{h}_t + \mathbf{P}\mathbf{F}\mathbf{P}_I\mathbf{v}_I + \mathbf{P}\mathbf{w}_f \tag{3}$$

where $\mathbf{v}_I$ contains all the N_I impulsive noise samples in one OFDM block, $\mathbf{P}$ is an $N_p \times N_c$ matrix taking N_p pilot subcarriers out of the total N_c subcarriers, and $\mathbf{P}_I$ is an $N_c \times N_I$ matrix containing the positions of the N_I impulsive noise samples. By choosing a suitable threshold parameter η through exiting works, the threshold test is utilized to obtain the positions of impulsive noise. We introduce a vector $\mathcal{I}_I$ to denote the positions of impulsive noise which satisfies

$$|r_t(\mathcal{I}_I(i))|^2 > G\eta, \quad i = 1, \dots, N_I \tag{4}$$

where G is the average power of the received signals. After obtaining $\mathcal{I}_I$, we can express $\mathbf{P}_I$ as

$$\mathbf{P}_I[i,k] = \begin{cases} 1, & i = \mathcal{I}_I(k), \quad k = 1, \dots, N_I \\ 0, & \text{otherwise} \end{cases}. \tag{5}$$

The GAMP algorithm is utilized to estimate the impulsive noise. We assume that the impulsive noise $\mathbf{v}_I = [v_1, \dots, v_{N_I}]^T$ has an L-component GM distribution with a probability density function (pdf) of

$$p(v_n; \mathbf{q}_v) = (1-\lambda_v)\delta(v_n) + \lambda_v \sum_{l=1}^{L} \omega_{v,l}\mathcal{N}(v_n; \theta_{v,l}, \phi_{v,l}) \tag{6}$$

where $\mathbf{q}_v \triangleq [\lambda_v, \boldsymbol{\omega}_v, \boldsymbol{\theta}_v, \boldsymbol{\phi}_v]^T$, $\boldsymbol{\omega}_v = [\omega_{v,1}, \dots, \omega_{v,L}]^T$, $\boldsymbol{\theta}_v = [\theta_{v,1}, \dots, \theta_{v,L}]^T$, $\boldsymbol{\phi}_v = [\phi_{v,1}, \dots, \phi_{v,L}]^T$, λ_v is the sparsity rate, $\delta(\cdot)$ is the Dirac delta, $\omega_{v,l}$ is the weight of the lth component, and $\mathcal{N}(v_n; \theta_{v,l}, \phi_{v,l})$ stands for the pdf of a Gaussian variable v_n with mean $\theta_{v,l}$ and variance $\phi_{v,l}$. Here $(\cdot)^T$ denotes transpose.

We adopt the GAMP approach to estimate the approximated posterior of impulsive noise [12]

$$p(v_n|\mathbf{r}_p; \mathbf{q}_v) = \frac{p(v_n; \mathbf{q}_v)\mathcal{N}(v_n; \hat{r}_n, \mu_n^r)}{\int_v p(v; \mathbf{q}_v)\mathcal{N}(v; \hat{r}_n, \mu_n^r)} \tag{7}$$

where $\hat{r}_n$ and μ_n^r are given in Algorithm 1. By substituting (6) into (7), the posterior of v_n can be obtained as

$$p(v_n|\mathbf{r}_p; \mathbf{q}_v) = (1-\pi_n)\delta(v_n) + \pi_n \sum_{l=1}^{L} \overline{\beta}_{n,l}\mathcal{N}(v_n; \gamma_{n,l}, \nu_{n,l}) \tag{8}$$

where

$$\overline{\beta}_{n,l} = \frac{\beta_{n,l}}{\sum_{k=1}^{L}\beta_{n,k}} \tag{9}$$

$$\beta_{n,l} = \lambda_v\omega_{v,l}\mathcal{N}(\hat{r}_n; \theta_{v,l}, \phi_{v,l} + \mu_n^r) \tag{10}$$

$$\nu_{n,l} = (1/\mu_n^r + 1/\phi_{v,l})^{-1} \tag{11}$$

$$\gamma_{n,l} = (\hat{r}_n/\mu_n^r + \theta_{v,l}/\phi_{v,l})\nu_{n,l} \tag{12}$$

$$\pi_n = \left(1 + \frac{(1-\lambda_v)\mathcal{N}(0; \hat{r}_n, \mu_n^r)}{\sum_{l=1}^{L}\beta_{n,l}}\right)^{-1}. \tag{13}$$

We apply the EM algorithm to learn the parameters in $\mathbf{q}_v$ iteratively. At the $(i+1)$th iteration, the EM update for λ_v is

$$\lambda_v^{(i+1)} = \arg\max_{0<\lambda_v<1} \sum_{n=1}^{N_I} E\Big\{\ln p(v_n; \lambda_v, \mathbf{q}_{v\backslash\lambda_v}^{(i)})|\mathbf{r}_p; \mathbf{q}_v^{(i)}\Big\} \tag{14}$$

where the superscript (i) denotes variables at the ith iteration, $\mathbf{q}_{v\backslash\lambda_v}^{(i)}$ represents λ_v being removed from $\mathbf{q}_v^{(i)}$(similar for other parameters later on). For $l = 1, \dots, L$, the EM updates of $\theta_{v,l}$, $\phi_{v,l}$ and $\omega_{v,l}$ are given by

$$\theta_{v,l}^{(i+1)} = \arg\max_{\theta_{v,l}\in\mathbb{R}} \sum_{n=1}^{N_I} E\Big\{\ln p\big(v_n; \theta_{v,l}, \mathbf{q}_{v\backslash\theta_{v,l}}^{(i)}\big)\big|\mathbf{r}_p; \mathbf{q}_v^{(i)}\Big\} \tag{15}$$

$$\phi_{v,l}^{(i+1)} = \arg\max_{\phi_{v,l}>0} \sum_{n=1}^{N_I} E\Big\{\ln p\big(v_n; \phi_{v,l}, \mathbf{q}_{v\backslash\phi_{v,l}}^{(i)}\big)\big|\mathbf{r}_p; \mathbf{q}_v^{(i)}\Big\} \tag{16}$$

$$\omega_{v,l}^{(i+1)} = \arg\max_{\substack{w_{v,l}>0;\\ \sum_l w_{v,l}=1}} \sum_{n=1}^{N_I} E\Big\{\ln p\big(v_n; \omega_{v,l}, \mathbf{q}_{v\backslash w_{v,l}}^{(i)}\big)\big|\mathbf{r}_p; \mathbf{q}_v^{(i)}\Big\}. \tag{17}$$

After subtracting the estimated impulsive noise $\hat{\mathbf{v}}_I$ from the received signals, the resulting signals on all subcarriers and the pilot subcarriers can be written respectively as

$$\bar{\mathbf{r}}_f = \mathbf{r}_f - \mathbf{F}\hat{\mathbf{P}}_I\hat{\mathbf{v}}_I \tag{18}$$

$$\bar{\mathbf{r}}_p \approx \mathbf{P}\mathbf{D}\mathbf{F}\mathbf{h}_t + \mathbf{P}\mathbf{w}_f \tag{19}$$

Algorithm 1 The GAMP algorithm [13]

Definition:

$\mathbf{y} = \mathbf{A}\mathbf{x} + \mathbf{w}$, $\mathbf{z} = \mathbf{A}\mathbf{x}$, $\mathbf{w}$ is additive Gaussian noise.

$p(z_m|\mathbf{y}; \hat{p}, \mu^p) = \frac{p(y_m|z_m)\mathcal{N}(z_m;\hat{p},\mu^p)}{\int_{z'_m} p(y_m|z'_m)\mathcal{N}(z'_m;\hat{p},\mu^p)}$

$p(x_n|\mathbf{y}; \hat{r}, \mu^r) = \frac{p(x_n)\mathcal{N}(x_n;\hat{r},\mu^r)}{\int_{x'_n} p(x'_n)\mathcal{N}(x'_n;\hat{r},\mu^r)}$

Input:

$p(x_n)$, $p(y_m|z_m)$, $\mathbf{A}$, T_{max}

Initialize:

$\forall n : \hat{x}_n(1) = \int_{x_n} x_n p(x_n)$

$\forall n : \mu_n^x(1) = \int_{x_n} |x_n - \hat{x}_n(1)|^2 p(x_n)$

$\forall m : \hat{s}_m(0) = 0$

for $t = 1 : T_{max}$

$\forall m : \mu_m^p(t) = \sum_{n=1}^{N} |A_{mn}|^2 \mu_n^x(t)$

$\forall m : \hat{p}_m(t) = \sum_{n=1}^{N} A_{mn}\hat{x}_n(t) - \mu_m^p(t)\hat{s}_m(t-1)$

$\forall m : \mu_m^z(t) = \mathrm{var}\{z_m|\mathbf{y}; \hat{p}_m(t), \mu_m^p(t)\}$

$\forall m : \hat{z}_m(t) = \mathrm{E}\{z_m|\mathbf{y}; \hat{p}_m(t), \mu_m^p(t)\}$

$\forall m : \mu_m^s(t) = (1 - \mu_m^z(t)/\mu_m^p(t))/\mu_m^p(t)$

$\forall m : \hat{s}_m(t) = (\hat{z}_m(t) - \hat{p}_m(t))/\mu_m^p(t)$

$\forall n : \mu_n^r(t) = (\sum_{m=1}^{M} |A_{mn}|^2 \mu_m^s(t))^{-1}$

$\forall n : \hat{r}_n(t) = \hat{x}_n(t) + \mu_n^r(t) \sum_{m=1}^{M} A_{mn}^* \hat{s}_m(t)$

$\forall n : \mu_n^x(t+1) = \mathrm{var}\{x_n|\mathbf{y}; \hat{r}_n(t), \mu_n^r(t)\}$

$\forall n : \hat{x}_n(t+1) = \mathrm{E}\{x_n|\mathbf{y}; \hat{r}_n(t), \mu_n^r(t)\}$

end

Output:

$\{\hat{z}_m(t), \mu_m^z(t)\}, \{\hat{r}_n(t), \mu_n^r(t)\}, \{\hat{x}_n(t+1), \mu_n^x(t+1)\}$

where $\hat{\mathbf{P}}_I$ is the estimation of $\mathbf{P}_I$. As the impact of impulsive noise is mitigated, the estimation of channel $\mathbf{h}_t$ is more accurate from (19). Similarly, the distribution of $\mathbf{h}_t = [h_1, \ldots, h_{N_c}]^T$ is considered to follow the GM model as

$$p(h_m; \mathbf{q}_h) = (1 - \lambda_h)\delta(h_m) + \lambda_h \sum_{l=1}^{L} \omega_{h,l}\mathcal{N}(h_m; \theta_{h,l}, \phi_{h,l}) \tag{20}$$

where $\mathbf{q}_h \triangleq [\lambda_h, \boldsymbol{\omega}_h, \boldsymbol{\theta}_h, \boldsymbol{\phi}_h]^T$, $\boldsymbol{\omega}_h = [\omega_{h,1}, \ldots, \omega_{h,L}]^T$, $\boldsymbol{\theta}_h = [\theta_{h,1}, \ldots, \theta_{h,L}]^T$, and $\boldsymbol{\phi}_h = [\phi_{h,1}, \ldots, \phi_{h,L}]^T$. Then, the posterior of $\mathbf{h}_t$, i.e., $p(h_m|\bar{\mathbf{r}}_p; \mathbf{q}_h)$ can be estimated similar to (8), where the parameters of $\mathbf{q}_h$ are learned through the EM approach, using the GAMP for the expectation step.

After estimating $\mathbf{h}_t$, we decode the transmitted bits through channel equalization and demodulation. The estimated bits are utilized to restore the transmitted OFDM symbol $\breve{\mathbf{d}}$ after modulation and pilot symbols insertion [14]. Then, $\breve{\mathbf{d}}$ is subtracted from the receive signals. Note that by eliminating the effect of the transmitted signals, the impulsive noise can be estimated more accurately. Such iterative estimation of $\mathbf{h}_t$ and $\mathbf{v}_I$ continues for a predetermined number of iterations.

IV. Simulation Results

In this section, the performance of the proposed algorithm is studied through numerical simulations. In the simulations, the UA channel is assumed to have 15 paths, and the arrival times of all paths follow a Poisson distribution with an average delay of 1 ms between two adjacent paths. The amplitudes of the paths are considered as Rayleigh distributed, whose variances decrease with an exponential profile. We use $\mathbf{u} = \mathbf{v}_t + \mathbf{w}_t$ to denote the total additive noise in (1) and the two-component GM model [15] is used to generate $\mathbf{u}$ with a pdf of

$$f(u[i]) = (1-q)\mathcal{N}(u[i]; 0, \sigma^2) + q\mathcal{N}(u[i]; 0, \sigma_I^2) \quad i = 1, \ldots, N_c \tag{21}$$

where σ^2 and σ_I^2 are the variances of the background noise and the impulsive noise, respectively, and q is the probability of occurrence of impulsive noise. In the simulations, we choose $q = 0.02$ and $\sigma_I^2/\sigma^2 = 400$.

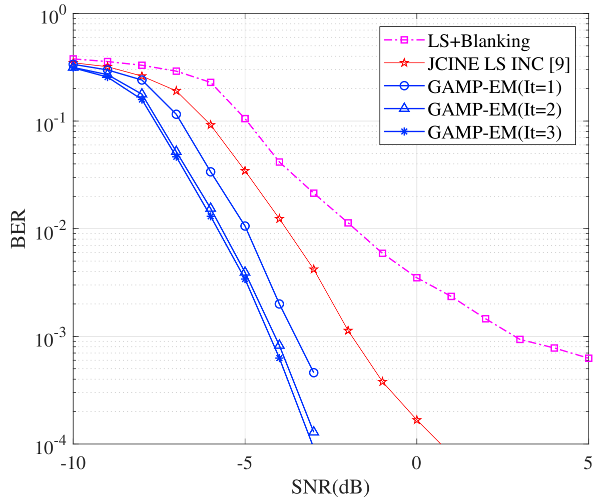

Fig. 1. BER Performance of various algorithms versus SNR.

The BER of the LS+blanking algorithm, the JCINE LS INC algorithm [9] and the proposed GAMP-EM algorithm versus SNR is shown in Fig. 1. We can see from Fig. 1 that the proposed algorithm achieves a lower BER than the existing methods. In particular, compared with the JCINE LS INC algorithm, the proposed algorithm has a gain of approximately 3.5 dB after three iterations. We can also observe from Fig. 1 that as the number of iterations increases, the performance improvement of the proposed algorithm decreases, especially at the third iteration. This reflects the typical diminishing return for iterative channel estimation algorithms. Considering the performance-complexity tradeoffs, two iterations of the proposed algorithm would be sufficient in practical UA OFDM systems.

V. Experimental Results and Discussions

In this section, the proposed algorithm is applied to process the real data collected during a UA communication experiment conducted in December 2015 in the estuary of the Swan River, Western Australia. The distance of the transmitter and receiver was 936 meters as shown in Fig. 2. As the receiver hydrophone and the transmitter transducer were mounted on steel frames, the movement of them was small, causing negligible Doppler shifts. Since the hydrophone was located in warm shallow water close to a jetty, the sources of impulsive noise consist

Fig. 2. Transmitter and receiver locations during the experiment.

TABLE I
EXPERIMENTAL SYSTEM PARAMETERS

Number of OFDM blocks	N_b	5
Number of total subcarriers	N_c	512
Number of data subcarriers	N_s	325
Number of pilot subcarriers	N_p	128
Number of null subcarriers	N_n	36
Number of subcarriers for frequency offset estimation	N_f	23
Carrier frequency	f_c	12 kHz
Bandwidth	B	4 kHz
Length of OFDM symbol	T_{sc}	128 ms
Length of CP	T_{cp}	25 ms

of highly impulsive snapping shrimp noise and breaking wave noise which is generated by waves breaking at the jetty piers. The key parameters of the experimental system are shown in Table I. During the experiment, we sent 500 frames in each transmission. The data symbols of the first 250 frames are encoded by $1/3$ rate turbo codes and the remaining 250 frames are encoded by $1/2$ rate turbo codes. The pilot symbols and the data symbols are modulated by QPSK constellations. Thus, each frame contains either 1632 information bits ($1/2$ rate code) or 1088 information bits ($1/3$ rate code). Under different wind conditions, we transmitted the same data file three times to study the effect of wind on the breaking wave noise whose intensity increases with the wind speed. The received data files were named T83, T84, and T85, respectively. The signals in the T83 file were slightly impacted by impulsive noise, and the signals in the T84 file were seriously interfered by impulsive noise.

The proposed GAMP-EM algorithm is utilized to process the received signals. The raw BER, coded BER, and FER performances of the following algorithms for the T83, T84, and T85 files are shown in Table II-IV, respectively.

- LS channel estimator after blanking of the impulsive noise detected at the positions of $\mathcal{I}_I$.
- JCINE algorithm with LS based INC [9].
- Proposed GAMP-EM algorithm at the first three iterations.

TABLE II
PERFORMANCE COMPARISON FOR THE T83 FILE

Coding rate	Method	Raw BER	Coded BER	FER
1/3	LS+blanking	5.2%	0%	0%
	JCINE LS INC	3.5%	0%	0%
	GAMP-EM (It=1)	3.7%	0%	0%
	GAMP-EM (It=2)	2.8%	0%	0%
	GAMP-EM (It=3)	2.3%	0%	0%
1/2	LS+blanking	4.7%	0%	0%
	JCINE LS INC	3.3%	0%	0%
	GAMP-EM (It=1)	3.4%	0%	0%
	GAMP-EM (It=2)	2.7%	0%	0%
	GAMP-EM (It=3)	2.3%	0%	0%

TABLE III
PERFORMANCE COMPARISON FOR THE T84 FILE

Coding rate	Method	Raw BER	Coded BER	FER
1/3	LS+blanking	15.5%	1.3%	7.3%
	JCINE LS INC	14.7%	0.5%	4.1%
	GAMP-EM (It=1)	13.3%	0.07%	0.4%
	GAMP-EM (It=2)	12.0%	0%	0%
	GAMP-EM (It=3)	11.5%	0%	0%
1/2	LS+blanking	14.6%	15.9%	84.7%
	JCINE LS INC	13.5%	11.1%	62.9%
	GAMP-EM (It=1)	12.4%	5.4%	34.6%
	GAMP-EM (It=2)	11.2%	2.4%	16.3%
	GAMP-EM (It=3)	10.7%	1.8%	12.6%

Since the signals in the T83 file are least interfered by impulsive noise, it can be seen from Table II that all three algorithms can achieve 0% coded BER and FER for the recorded data. Moreover, the proposed algorithm can obtain a lower raw BER than the other two algorithms.

For the T84 file, it can be seen from Table III that compared with existing approaches, after two iterations, the proposed algorithm can achieve 0% FER for the recorded $1/3$ rate signals. Compared with the LS+blanking method, the proposed algorithm reduces the coded BER from 1.3% to 0% for the $1/3$ rate signals and from 15.9% to 1.8% for the $1/2$ rate signals. As the T84 file is heavily affected by impulsive noise, for the $1/2$ rate signals, the FER of the JCINE LS INC algorithm is much higher than the proposed algorithm.

TABLE IV
PERFORMANCE COMPARISON FOR THE T85 FILE

Coding rate	Method	Raw BER	Coded BER	FER
1/3	LS+blanking	11.3%	0%	0%
	JCINE LS INC	9.1%	0%	0%
	GAMP-EM (It=1)	9.0%	0%	0%
	GAMP-EM (It=2)	7.5%	0%	0%
	GAMP-EM (It=3)	6.9%	0%	0%
1/2	LS+blanking	11.6%	3.8%	24.2%
	JCINE LS INC	9.8%	0.6%	5.7%
	GAMP-EM (It=1)	9.7%	0.5%	3.3%
	GAMP-EM (It=2)	8.6%	0%	0%
	GAMP-EM (It=3)	7.9%	0%	0%

As the signals in the T85 file are moderately impacted by impulsive noise, the results in Table IV show that all three algorithms can achieve 0% coded BER and FER for the recorded $1/3$ rate signals. However, compared with the JCINE LS INC algorithm, the proposed algorithm has 2.2% reduction in the raw BER for the $1/3$ rate signals. For the $1/2$ rate signals, the proposed algorithm has 1.9% decrease in the raw BER, 0.6% decrease in the coded BER, and 5.7% decrease in the FER after three iterations. The results in Tables II-IV indicate that the proposed algorithm can better recover the transmitted signals than existing approaches.

VI. Conclusion

In this paper, we propose a novel algorithm to mitigate the impulsive noise and estimate the channel impulse response of UA OFDM systems. By considering the prior information, the GAMP algorithm is utilized to estimate the posteriors of the impulsive noise and the channel impulse response. The EM method is used to compute the optimal parameters. To make full use of the receive signals, we iteratively estimate the channel and the impulsive noise. The simulation and experimental results show that the proposed algorithm achieves a lower BER and FER than existing algorithms, even when the transmitted signals are severely interfered by impulsive noise.

References

[1] A. C. Singer, J. K. Nelson, and S. S. Kozat, "Signal processing for underwater acoustic communications," *IEEE Commun. Magazine*, vol. 47, no. 1, pp. 90-96, Jan. 2009.

[2] P. Qarabaqi and M. Stojanovic, "statistical characterization and computationally efficient modeling of a class of underwater acoustic communication channels," *IEEE J. Oceanic Engineering*, vol. 38, no. 4, pp. 701-717, Oct. 2013.

[3] J. Hildebrand, "Anthropogenic and natural sources of ambient noise in the ocean," *Mar. Ecol. Progr. Ser.*, vol. 395, pp. 5-20, Dec. 2009.

[4] A. Chang, Y. Cheng, C. Chen, H. Chan, and S. Lin, "Modeling of shallow water ambient noise based on adiabatic mode theory," in *Proc. IEEE Int. Underwater Technology Symposium*, Tokyo, Japan, Mar. 2013, pp. 1-5.

[5] M. Stojanovic, "Low complexity OFDM detector for underwater acoustic channels," in *Proc. IEEE OCEANS*, Boston, USA, Sep. 2006.

[6] T. Suzuki, H. M. Tran, and T. Wada, "An underwater acoustic OFDM communication system with shrimp (impulsive) noise cancelling," in *Proc. Int. Conf. Computing, Management, Telecommun.*, Da Nang, Vietnam, Apr. 2014, pp. 152-156.

[7] T. Y. Al-Naffouri, A. A. Quadeer, and G. Caire, "Impulse noise estimation and removal for OFDM systems," *IEEE Trans. Commun.*, vol. 62, no. 3, pp. 976-989, Mar. 2014.

[8] W. Li and J. C. Preisig, "Estimation and equalization of rapidly varying sparse acoustic communication channels," in *Proc. MTS/IEEE OCEANS*, Boston, MA, USA, Sep. 2006, pp. 1-6.

[9] P. Chen, Y. Rong, S. Nordholm, Z. He, and A. Duncan, "Joint channel estimation and impulsive noise mitigation in underwater acoustic OFDM communication systems," *IEEE Trans. Wireless Commun.*, vol. 16, pp. 6165-6178, Sep. 2017.

[10] P. Chen, Y. Rong, S. Nordholm, and Z. He, "Joint channel and impulsive noise estimation in underwater acoustic OFDM systems," *IEEE Trans. Veh. Technol.*, vol. 66, no. 11, pp. 10567-10571, Nov. 2017.

[11] S. Wang, Z. He, K. Niu, P. Chen, and Y. Rong, "A sparse Bayesian learning based joint channel and impulsive noise estimation algorithm for underwater acoustic OFDM systems," in *Proc. MTS/IEEE OCEANS*, Kobe, Japan, May 28-31, 2018.

[12] J. P. Vila and P. Schniter, "Expectation-maximization Gaussian-mixture approximate message passing," *IEEE Trans. Signal Process.*, vol. 61, no. 19, pp. 4658-4672, Oct. 2013.

[13] S. Rangan, "Generalized approximate message passing for estimation with random linear mixing," in *Proc. IEEE ISIT*, Saint-Petersburg, Russia, July. 31-Aug. 5, 2011, pp. 2168-2172.

[14] J. Zhang, Z. He, P. Chen, and Y. Rong, "A compressive sensing based iterative algorithm for channel and impulsive noise estimation in underwater acoustic OFDM systems," in *Proc. MTS/IEEE OCEANS*, Anchorage, AK, USA, Sep. 2017, pp. 1-5.

[15] X. Kuai, H. Sun, S. Zhou, and E. Cheng, "Impulsive noise mitigation in underwater acoustic OFDM systems," *IEEE Trans. Veh. Technol.*, vol. 65, no. 10, pp. 8190-8202, Oct. 2016.